Facial Nerve Tractography

in patients with vestibular schwannomas

18-11-2024

Wouter Maathuis

Master Thesis, Technical Medicine

UNIVERSITY OF TWENTE.

UMC Utrecht

Acknowledgements

I have spend the past year working on my master thesis at the department of neurosurgery of the UMC Utrecht. Throughout the year, I was fortunate enough to receive the help of a lot of supervisors and colleagues. They did not only help me with the project, but also brought a lot of fun with them.

First of all, I would like to thank the members of my graduation committee for their time and expertise throughout the year. Of course, Tessa and Tristan for all of your time and effort getting me integrated into the department and your daily and clinical guidance. Bennie, you always helped me to take a step back and appreciate the value of my work. And finally Lieke, for your help and stimulation regarding my personal development during the thesis together with our intervision group.

Apart for my graduation committee, I would also like to thank everybody at the neurosurgical department, Anouk in particular, for helping me with the further development of my clinical skills, as well as with navigating the hospital logistics and bureaucracy. Besides, I want to thank everyone at AugmedIT for new perspectives and insights on the Wednesdays. A special thanks to Alexander, Alberto and Niels for their expertise and help regarding the acquisition and processing of diffusion MRI. I would also like to thank Eduard and Hans for their willingness to work with me on this project, and to test the findings in a clinical setting. A final thanks to the members of the research group (Mathijs, Jesse, Jari, Kevin, Elisa, Manon and Hidde) for all of your help and above all fun throughout the year.

You all not only helped me give shape to the project, but also contributed to my enjoyment of the year!

Wouter Maathuis

Utrecht, November 2024

Graduation committee

Chairman	B. ten Haken Prof. PhD. Ir.
Medical supervisor	T. van Doormaal, MD, PhD
Technical Medicine supervisor	T.M. Kos, MSc
Technical supervisor UT	B. ten Haken Prof. PhD. Ir.
Process supervisor UT	L. Menzing-Folsche, MSc
External member	B. Wermelink, PhD

Table of contents

Abbreviations

AR	Augmented reality
dMRI	Diffusion MRI
DTI	Diffusion tensor imaging
DWI	Diffusion weighted imaging
FA	Fractional anisotropy
FLAIR	Fluid-attenuated inversion recovery
IQR	Interquartile range
PGSE	Pulsed gradient spin echo
ROI	Region of interest
SNR	Signal-to-noise ratio
T1c	T1-weighted MRI scan with contrast (gadolinium)
VS	Vestibular schwannoma

Clinical background

Vestibular schwannoma's (VSs) are benign tumors originating from the Schwann cells surrounding the vestibulocochlear nerve. They account for approximately 8% of all intracranial tumors [1]. Patients presenting with VSs often show otological symptoms such as progressive sensorineural hearing loss, unilateral tinnitus, and vertigo [2]. Large VSs can cause brainstem compression, which can result in additional symptoms such as hydrocephalus, dysmetria and facial nerve impairment [1].

Diagnostics

The primary indication for VS screening with magnetic resonance imaging (MRI) is sudden or asymmetric sensorineural hearing loss [1]. Contrast-enhanced T1-weighted sequences (T1c) are considered to be the gold standard for initial assessment and postoperative evaluation of the lesion [3]. According to literature, the MRI protocol should also include standard T1- and T2-weighted scans, diffusion-weighted imaging (DWI) and fluid-attenuated inversion recovery (FLAIR) sequences. These different sequences help to differentiate between diagnoses. Based on imaging, the VS is graded according to the Koos grading scale (Table 1)[4].

Table 1: Koos grading scale for vestibular schwannomas.

Grade	Description
I	Small intracanalicular tumor.
II	Small tumor with protrusion into the cerebellopontine cistern; no contact with brainstem.
III	Tumor occupying the cerebellopontine cistern with no brainstem displacement
IV	Tumor with brainstem and cranial nerve displacement

Treatment

The treatment options for VSs after diagnosis are conservative treatment, radiotherapy, surgical resection or a combination. Conservative treatment is only possible if the growth rate of the tumor is low and the patient is asymptomatic. Radiotherapy aims at minimizing the growth rate of the tumor. In case the VS is of such size that it causes mass effect (Koos grade IV), surgical intervention is advised [2], [5].

Surgery

Surgical intervention aims at maximizing tumor tissue resection whilst preserving neurological function. Primary surgical risks are postoperative hearing deficits and facial nerve malfunction. Intraoperative neuromonitoring, consisting of evoked potentials and direct electrical stimulation, is used for the identification of the facial nerve and is mandatory to minimize damage [3]. Patients with tumors smaller than 15 mm will have an average chance of facial nerve damage (House-Brackman grade III or above, Table 2) of 8%, whereas this number increases to 36% for tumors larger than 30 mm [6].

Table 2: House-Brackmann scale for facial nerve function [7].

Grade	Definition
I	Normal symmetrical function in all areas
II	Slight weakness noticeable only on close inspection. Complete eye closure with minimal effort. Synkinesis barely noticeable, contracture or spasm absent.
III	Obvious weakness, but not disfiguring. May not be able to lift eyebrow. Complete eye closure and strong but asymmetrical mouth. Movement with maximal effort. Obvious, but not disfiguring synkinesis, mass movement or spasm.
IV	Obvious disfiguring weakness. Inability to lift eyebrow. Incomplete eye closure and asymmetry of mouth with maximal effort. Severe synkinesis, mass movement, spasm.
V	Motion barely perceptible. Incomplete eye closure, slight movement corner of mouth.
VI	No movement, loss of tone, no synkinesis, contracture of spasm.

It is expected that this risk of facial nerve damage can be further reduced when the neurosurgeon is aware of the trajectory of the facial nerve prior to surgery [8]. Obtaining this information could allow for faster surgeries and potentially reduce the surgical experience needed to perform the intervention [9]. However, conventional MRI sequences do not result in intensity differences between the lesion and facial nerve, making it impossible to identify it [10], [11].

Diffusion MRI

Diffusion weighted imaging (DWI) with MRI (or diffusion MRI) is an imaging sequence which is weighted according to the diffusion of water. It is based on a pulsed gradient spin echo (PGSE) sequence, which uses diffusion sensing gradients to de- and rephase spins [12]. Stationary spins are unaffected, however diffusing spins migrate and consequently fall out of phase which leads to signal loss. This can be characterized in Equation 1.

Equation 1

$$S = S_0 * e^{-b*D}$$

Where S is the signal intensity, S_0 is the baseline signal intensity, D is the diffusion coefficient [mm^2/s], and b the b-value [s/mm^2]. The b-value depends on the strength, duration, and spacing of the diffusion gradients, and is typically in the range of 0 to 4000 s/mm^2.

Diffusion tensor imaging (DTI)

Diffusion can be modelled with a diffusion tensor (D), which is an array of numbers corresponding to the average directional diffusion coefficients within one voxel (Equation 2). An minimum of 6 diffusion gradient directions needs to be included in the DWI sequence to properly estimate the diffusion tensor, but on average 30 different directions are recommended [13]. In case of isotropic diffusion ($D_{isotropic}$), the diffusion is the same in all directions.

Equation 2

$$\text{Diffusion tensor (D)} = \begin{bmatrix} Dxx & Dxy & Dxz \\ Dyx & Dyy & Dyz \\ Dzx & Dzy & Dzz \end{bmatrix}, D_{isotropic} = \begin{bmatrix} D & 0 & 0 \\ 0 & D & 0 \\ 0 & 0 & D \end{bmatrix}$$

In DTI, the diffusion tensor is approximated and converted into the optimal frame of reference, which is parallel to the principal diffusion direction in one voxel. The principal diffusion direction is often specific to certain tissues, such as white matter tracts and facial planes. There are two additional diffusion directions which are perpendicular to the principal direction and each other. These major and minor diffusion axes are described by eigenvectors (ε_1, ε_2, ε_3) and corresponding eigenvalues (λ_1, λ_2, λ_3). This removes the covariance between the x, y and z direction and consequently simplifies the estimated diffusion tensor to the one described in Equation 3.

Equation 3

$$\Lambda = \begin{bmatrix} \lambda 1 & 0 & 0 \\ 0 & \lambda 2 & 0 \\ 0 & 0 & \lambda 3 \end{bmatrix}$$

DTI post-processing

The estimated diffusion tensor can be visualised and post-processed in multiple ways. Three common approaches are fractional anisotropy (FA) maps, principal diffusion direction maps and fiber tracking maps.

FA is a measure for the asymmetry of the diffusion in a voxel. It is a scalar between 0 and 1, where perfect isotropic diffusion equates to a FA value of 0. If the diffusion tends to be in one direction, the FA will increase. This allows for the detection of anatomical structures with primarily unidirectional diffusion. It is calculated according to Equation 4.

Equation 4

$$FA = \sqrt{\frac{(\lambda 1 - \lambda 2)^2 + (\lambda 2 - \lambda 3)^2 + (\lambda 1 - \lambda 3)^2}{2(\lambda 1^2 + \lambda 2^2 + \lambda 3^2)}}$$

Principal diffusion direction maps visualize the anisotropy as well as the direction of the principal diffusion direction within a voxel. This is achieved by colour coding the images in such a way that these parameters are included. Usually, the orientation of ε_1 determines the hue and the FA value the brightness.

Fiber tracking maps are used to reconstruct nerve and/or white matter trajectories [14]. The reconstructions are based on both the FA as well as the principal diffusion direction (ε_1). Seed points are selected in addition to regions of interest (ROIs). Fiber trajectories which originate from this seed and also pass through the ROIs are calculated. In its most basic form, tractography follows the direction of ε_1 for each successive voxel until termination criteria are met. These criteria usually based on FA thresholds and angulation of the tract. It is important to note that the fiber tracking results are highly dependent on the seed point location, ROI selection and termination criteria. These often differ between observers, leading to varying results.

Application of MR-DTI in neurosurgery

MR-DTI is a popular tool to study white matter anatomy and architecture in vivo. The method has been implemented to study patients suffering from acute stroke, neurodegenerative disease and brain tumors [13]. Additionally, there have been multiple studies that investigated the ability of MR-DTI to compute the trajectory of the facial nerve in patients with VSs. A literature search was conducted, which included original research and reviews papers in which the use of DTI to visualize the facial nerve in patients with VSs was discussed. This section discusses these papers and recent reviews on the subject.

Facial nerve tractography

Taoka et al. were the first to use DTI-based tractography to visualize the facial nerve in patients with VSs [15]. More refined techniques and reconstruction algorithms have been developed over the years to improve upon their results [5], [16], [17], [18], [19], [20], [21], [22], [23], [24]. All of the studies investigating DTI of the facial nerve reconstructed the nerve trajectory prior to surgery and verified their computations intraoperatively. Third party software such as BrainLab iPlan (BrainLab, Feldkirchen, Germany), StealthViz (Medtronic Navigation, Louisville, CO, USA) and 3D Slicer [25] was used by all of them (except for Taoka et al.). All authors reported successful reconstructions with moderate to high correspondence to the intra-operative location. Only one study investigated the impact of facial nerve tractography on the complication rates in VS resection [24]. They concluded that although they could predict the facial nerve correctly in 81.6% of the patients, the accuracy of the reconstruction did not prevent facial palsy.

All DTI-based reconstructions of the facial nerve were visualised on workstations such as BrainLab iPlan and StealthStation (Medtronic Navigation, Louisville, CO, USA). In these software packages, the nerve trajectory was displayed in a common DICOM viewer fashion combining a 2D slice viewer with 3D trajectories. This was done with either 2D or 3D segmentations, or a combination of both. Only one author reported an additional visualization method: integration in the surgical microscope [24].

Two recent reviews included all abovementioned papers [9], [26]. They conclude that DTI-based tractography is a promising method to visualize facial nerve trajectories in patients with both small and large VSs (>2.5 cm). However, they stress that it requires experienced operators and that its clinical reproducibility is limited due to the highly operator-dependent results. The included studies varied in terms of acquisition parameters, software and post-processing parameters, leading to varying results. Due to this heterogeneity, no recommendations in terms of systems, settings or image processing are made for the usage of DTI. As a result, no large clinical studies investigating the clinical benefit of visualizing the facial nerve with DTI have been performed.

Research objectives

The aim of this study is to evaluate the feasibility of the clinical implementation of facial nerve tractography in patients with vestibular schwannomas. To investigate the feasibility of clinical implementation of this technology, we wanted to encompass the entire workflow: from MRI scan protocol selection to data presentation in the operating room. This provides a clinical context for the method, revealing its strengths and limitations. Consequently, we defined our primary and secondary study objectives as follows:

Primary:

To evaluate the feasibility of DTI-based tractography for facial nerve visualisation in the preoperative workflow of patients with vestibular schwannomas.

Secondary:

1. Determine if clinical DWI scans can be used to reconstruct non-pathological facial nerves.
2. Develop and evaluate a method for DTI-based tractography reconstructions of the facial nerve in patients with vestibular schwannomas.
3. Investigate the potential added value of AR for the visualisation and interpretation of facial nerve tractography.

CHAPTER 1

Non-pathological facial nerve reconstructions using clinical DWI scans

Introduction

Our first objective is to explore the feasibility of non-pathological facial nerve tractography using the clinical diffusion MRI (dMRI) protocol used in the preoperative workflow for neuro-oncological patients. The facial nerve tracts will be reconstructed using a tractography algorithm. The tract reconstructions are compared against the location of the nerve on the T2 FLAIR MRI scan, to assess the feasibility of the method and the data quality requirements.

Objective:

To evaluate the feasibility of non-pathological facial nerve tractography in glioma patients using the conventional clinical DWI protocol.

Methods

We retrospectively included glioma patients treated in the department of neurosurgery in the UMC Utrecht. Our aim was to include five patients with bilateral unaffected facial nerves. A 3 Tesla Philips Ingenia CS system was used to scan the patients the day before surgery, using the routine clinical scan protocol consisting of a three-dimensional (3D) T2-weighted FLAIR, 3D T1c and a dMRI scan. All patients were scanned with all sequences in one session. This was done according to the parameters summarized in Table 3.

Table 3: Dataset overview.

Scan	Voxel size (x, y, slice)[mm]	Slice thickness [mm]	TR [ms]	TE [ms]	TI [ms]	b-value	Diffusion gradients
DWI	2.30 x 2.30 x 3.00	3	5807	69	n.a.	800	16
FLAIR	0.744 x 0.744 x 0.56	1.12	4800	251.5	1650	n.a.	n.a.
T1c	0.744 x 0.744 x 0.75	1.5	7.8	3.7	n.a.	n.a.	n.a.

Data processing

A schematic overview of the data processing can be seen in Figure 1. All data was converted to the NIfTI format and loaded into 3D Slicer [25]. First, the left and right facial nerve were manually segmented from the original FLAIR scan. Next, the FLAIR scan was rigidly registered to the DWI scan, using the Elastix extension in 3D Slicer [27]. A marker was placed halfway down the intracranial trajectory of the left and right facial nerve on the registered FLAIR scan. These markers were imported into MATLAB (R2024a) and converted to binary region of interest (ROI) masks.

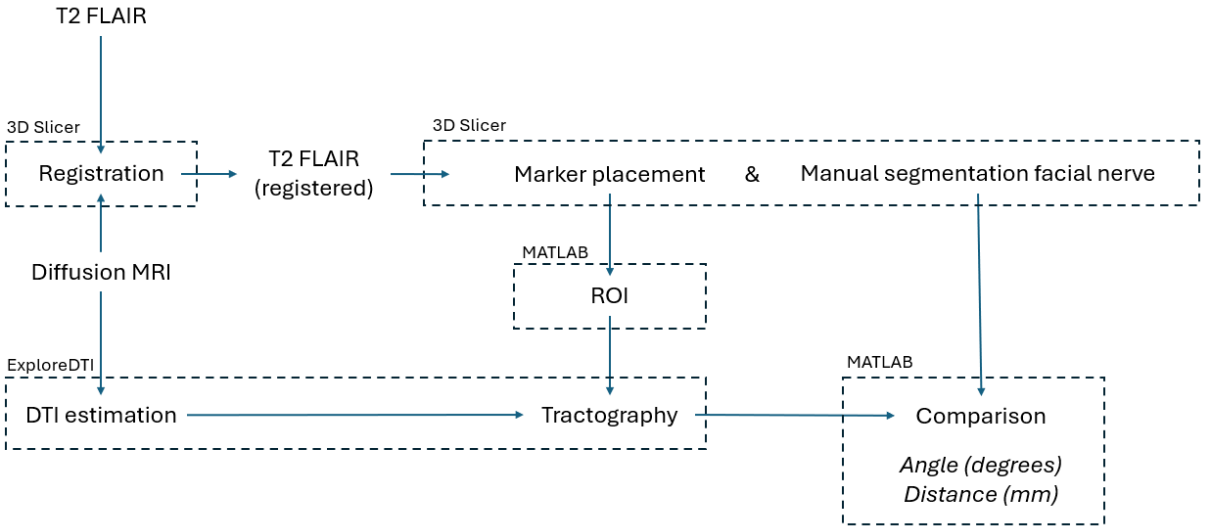

Figure 1: schematic overview of data processing.

Tractography

The DWI scan and ROI masks were imported into ExploreDTI [28], where the masks functioned as a seed ROI for the facial nerve reconstruction. The diffusion tensor was calculated for each voxel, and the integrated deterministic tractography algorithm [29] was used to generate tracts passing through the ROIs. The tractography parameters are summarized in Table 4.

Table 4: tractography parameters

Parameter	**Value**
Seedpoint resolution [mm]	2x2x2
FA threshold	0.1
Fiber length range [mm]	10-20
Angle threshold	45^0
Step size	1
Interpolation method	Linear

Comparison

The tractography results were compared to the facial nerve segmentation on the T2-FLAIR scan. For each facial nerve of each patient, the average distance between each reconstructed tract and the nerve segmentation was calculated. The average orientation, defined as the line between the most medial and most lateral point, was calculated for both the segmentations and tracts (Figure 2). The angle between these two lines indicated the difference in orientation between the segmentation and the tracts.

The best reconstruction was filtered out of all reconstructed tracts based on the distance and angle metric. If the angle of the tract closest to the FLAIR segmentation was below 20 degrees, it was considered to be the best reconstruction. Otherwise, the tract with a comparable distance but smaller angle was chosen.

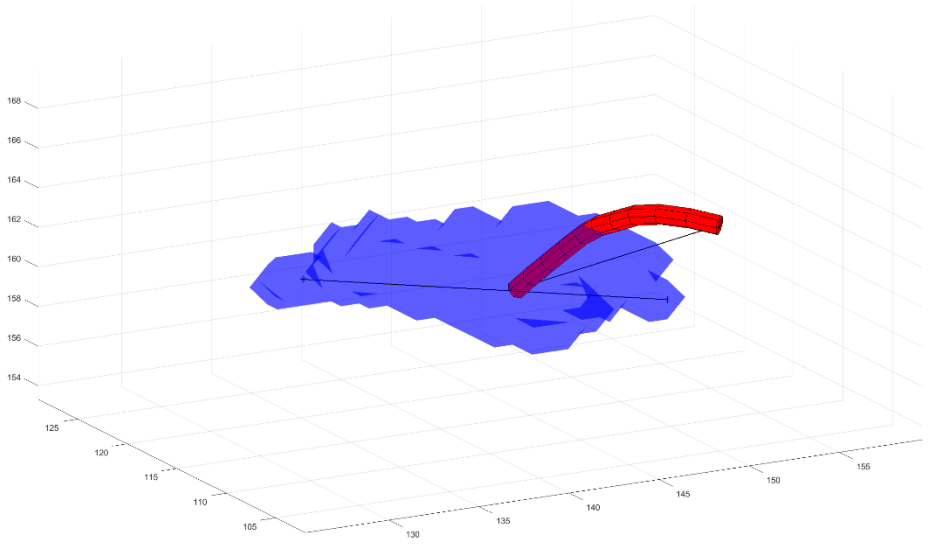

Figure 2: average orientation of segmented facialis (blue) and of tract (red) is defined by the most medial and most lateral point. The angle between these two lines (black) is calculated and reported.

Location validation

A validation step was included to rule out the occurrence of any coordinate shifts when passing data through the preprocessing and tractography pipeline. Two ROIs were used to evaluate these shifts. The first ROI was placed unilaterally in the medulla oblongata. With this ROI, the corticospinal tracts were reconstructed to evaluate shifts in the axial plane. The second was placed midsagittal in the anterior horn of the corpus callosum for the interhemispheric tracts, which were used for shifts in the sagittal plane. This way, the x, y and z direction are all incorporated in to the location validation.

The ROIs were drawn using 3D Slicer and converted to masks in MATLAB. The masks were used to reconstruct tracts using the same tractography parameters as for the facial nerve. Both the ROIs and corresponding reconstructed tracts were imported into MATLAB. For each tract, the minimum distance to the ROI was calculated. This distance was averaged over all tracts for each ROI in each patient (Figure 3).

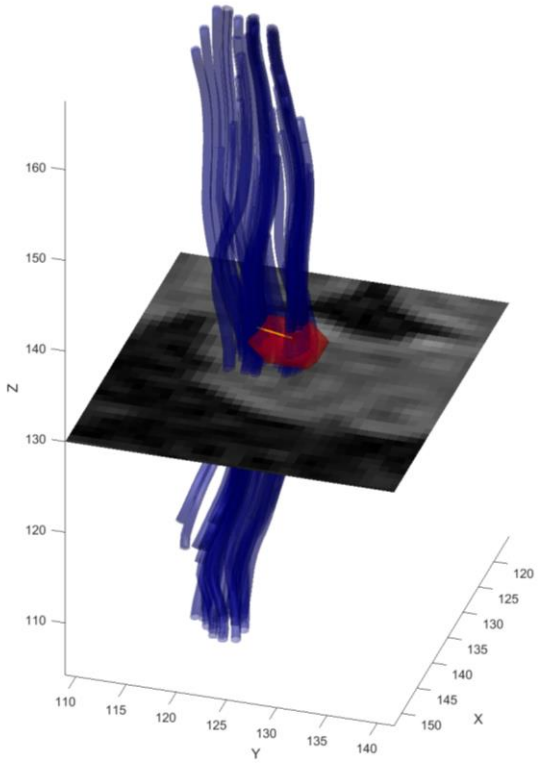

Figure 3: coördinate shift (yellow) defined as average distance between reconstructed tracts (blue) and ROI placed unilaterally in the medulla oblongata (red)

Results

Tract reconstruction, based on both the right and left ROI, was successful in all patients, for a total of 10 reconstructions. Across all reconstructions, the average distance to the segmentation was 1.43mm (95% CI, 0.8 – 2.0) and the average angle was 33.2 degrees (95% CI, 16.0 – 50.0). All results are summarised in Table 5.

Four outliers could be identified based on the distance and angle values. These are: P1-Left, P1-Right, P2-Right and P3-Left. An example is shown in Figure 4.

Table 5: distances and angles between tracts and segmentations.

Patient	**Average distance to facialis segmentation [mm]**	**Angle between segmentation and tract [°]**
P1 – Left	2.64	46
P1 – Right	1.99	50
P2 – Left	1.02	14
P2 – Right	1.71	88
P3 – Left	1.25	30
P3 – Right	2.76	9
P4 – Left	0.56	12

P4 – Right	1.35	39
P5 – Left	0.46	25
P5 – Right	0.51	19
Average	**1.43**	**33.2**
95% CI	**0.8 – 2.0**	**16.0 – 50.0**
Sigma	**0.8**	**24.0**

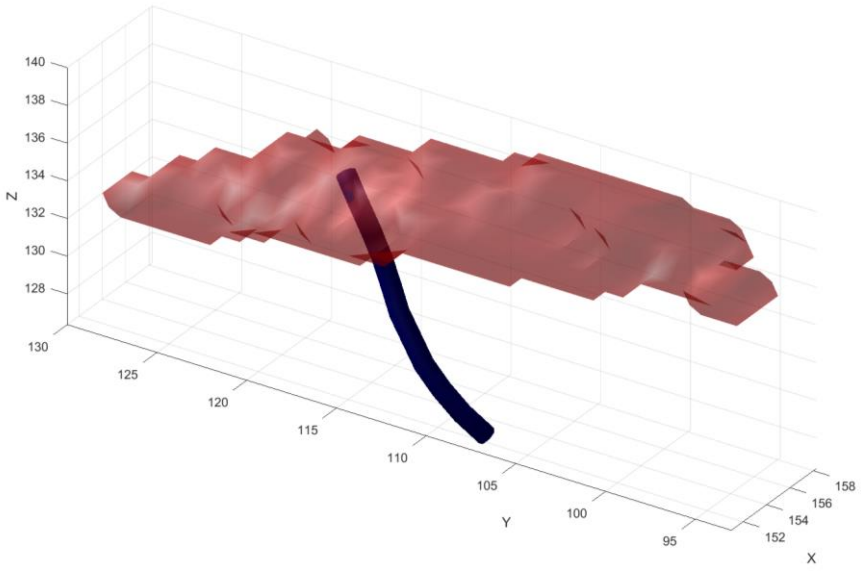

Figure 4: outlier example (P1-Left). The orientation of the reconstructed tract is completely different to the FLAIR segmentation.

For the validation ROIs, the average coordinate shift in the axial plane was 0.30mm (95% CI, 0.04 – 0.56) and in the sagittal plane 0.33mm (95% CI, 0.15 – 0.51). Table 6 summarize the results of the location validation.

Table 6: axial and sagittal shift.

Patient	Axial shift [mm]	Sagittal shift [mm]
1	0.21	0.17
2	0.01	0.48
3	0.31	0.48
4	0.38	0.31
5	0.58	0.22
Average	**0.30**	**0.33**
95% CI	**0.04 – 0.56**	**0.15 – 0.51**
Sigma	**0.21**	**0.14**

Discussion

In this chapter, we have shown that it is feasible to identify non-pathological facial nerves using DTI tractography. With our method, tract reconstruction using a clinical dMRI sequence was possible on bilateral facial nerves in all patients. On average, the reconstructions were located 1.43mm (95% CI, 0.8 – 2.0) away from the true nerve location with an average angle of 33.2 degrees (95% CI, 16.0 – 50.0). This distance was smaller than the voxel size of the DWI scan, on which the reconstructed tracts are based.

Four outliers could be identified mostly due to the large angles. These include: P1-Right, P1-Left, P2-Right and P3-Left. Upon visual inspection of these results, we could conclude that these reconstructions were unsuccessful. All were oriented similarly to P1-Left (Figure 4). Consequently, 6 out of 10 reconstructions can be deemed successful.

There are multiple possible explanations for the coordinate shift between the tract reconstructions and the segmentations. First of all, in can be an inherent part of the method. It is most likely that, in our method, the registration has the biggest influence on the coordinate alignment. We used the Elastix software to perform a rigid registration on the FLAIR and DWI scans [27]. We investigated its influence by calculating the distance between specific ROIs and the reconstructed tracts using the same tractography method. We found that shifts induces by the registration are small components of on average 0.32mm in the axial and sagittal planes.

Lastly, the parameters in the DWI sequence were not directly suitable for facial nerve reconstruction. The voxel size was large (2.3 x 2.3 x 3 mm) and anisotropic and there were few diffusion gradient directions. Facial nerve tractography is usually based on MR sequences with isotropic voxel sizes equal to or smaller than 2mm and 30 or more diffusion gradient directions [9]. Larger voxel sizes average the diffusion signal over a larger volume of tissue. This results in larger discontinuities in the principal diffusion axes and lowers the location certainty [14]. A smaller number of gradients will result in a less accurate calculation of the principal diffusion axis, on which tractography is based. Together, these factors could account for the location and angle deviations found in this study.

The choice of tractography algorithm and parameter settings are inherently a trade-off between sensitivity and specificity. In this study, we were able to allow a high false-positive rate since we could use the distance metric to filter them out. Without the ground truth (FLAIR segmentation), this filtering is not possible. So for clinical use, it is imperative to fine-tune the algorithm and parameter settings based on the specific use-case.

A final limitation of this study is that both the vestibulocochlear nerve and facial nerve were non-pathological. This is not fully representative of the final use-case in VS patients. Furthermore, both nerves contributed to the diffusion signal which could explain the location inaccuracy. It is therefore important to consider the possibility that the signal of the facial nerve alone could be insufficient for this reconstruction method.

Conclusion

It was possible to reconstruct the trajectories of non-pathological facial nerves with clinical diffusion scans using the conventional neuro-oncological scan parameters. However, sub-optimal scan parameters result in low precision reconstructions. For facial nerve localization in patients with VSs, it is recommended that the spatial and temporal resolution of the protocol are improved. This can be achieved by selecting a smaller voxel size and increasing the number of gradient directions in the dMRI protocol.

CHAPTER 2

Preoperative facial nerve visualisation in patients with vestibular schwannomas using DTI-based tractography

Introduction

The aim of this chapter is to determine the accuracy of facial nerve tractography in patients with vestibular schwannoma's. We use DTI-based tractography to reconstruct the course of the nerve. During surgery, the facial nerve location is identified and registered using the neuronavigation system. We compared the reconstructions against the intraoperative location to determine the accuracy of our method.

Objective: to develop and evaluate a method for DTI-based tractography reconstructions of the facial nerve in patients with vestibular schwannomas.

Methods

We included patients that were treated in the UMCU for surgical resection of vestibular schwannomas between February and September in 2024. A 3 Tesla scanner was used (Ingenia CS, Philips Medical Systems, Netherlands) to scan each patient the day before surgery. The collected scans were a regular presurgical neuronavigation scan (T1c, Table 7) as well as a custom dMRI sequence (Table 8).

Table 7: MRI sequence parameters.

Scan	Voxel size (x, y, slice)[mm]	Slice thickness [mm]	TR [ms]	TE [ms]
T1c	0.744 x 0.744 x 0.75	1.5	7.8	3.7

Two different DWI protocols were used (Table 8). We started with a research protocol which was developed by other researchers in our department. This allowed for an early start with patient inclusion. This protocol was fine-tuned after the inclusion of the first two patients, based on our findings in Chapter 1, literature and expert opinion (Appendix 1).

Table 8: acquisition parameters of diffusion protocols.

Protocol	Patients	Voxel size [mm]	Slice thickness [mm]	# Diffusion gradients	b-value [s/mm^2]	Notes
1	1 - 2	2 x 2 x 2.2	2.2	24+1	1000	Multi-shell
2	3 - 6	2 x 2 x 2	2	32+1	1000	-

During surgery, the facial nerve was localized either visually or with the neuromonitoring probe by the surgeon. After identification, a minimum of three points along the trajectory of the facial nerve was registered using the Brainlab neuronavigation system. The aim was to locate points at the brainstem, halfway down the tumor and at the porus.

Data processing

A schematic overview of the data processing is shown in Figure 5. The imaging data, consisting of the diffusion and T1c MRI scans, was uploaded to 3D Slicer [25] for pre-processing. The tumor, cerebellum and the entire brain were segmented automatically from the T1c scan using a deep-learning based method [30]. Two points were annotated on the T1c scan in the axial plane: point 1 on the anterior wall of the porus acousticus and point 2 on its posterior wall. Next, the T1c scan is registered to the diffusion scan using the Elastix plugin in 3D Slicer [27]. The segmented structures and the annotated points are transformed along with the T1c scan.

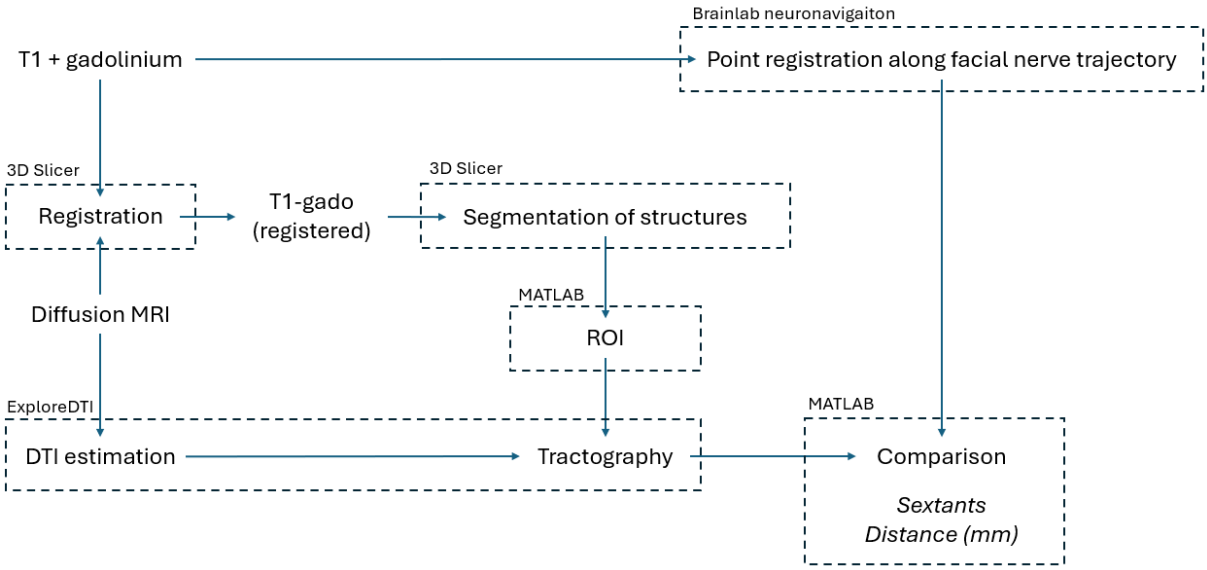

Figure 5: schematic overview of data processing.

The transformed points and segmentations were imported into MATLAB (R2024a). Using custom code, they were transformed into three ROIs for tractography (Figure 6). The first ROI was based on the annotated points. A square was created with sides equal to the distance between the two points. The square was oriented in such a way that the points are in the middle of the opposite sides.

The second ROI was based on a shell surrounding the tumor segmentation. The most medial third of this shell was used as the second ROI. The segmented cerebellum was used as the final ROI.

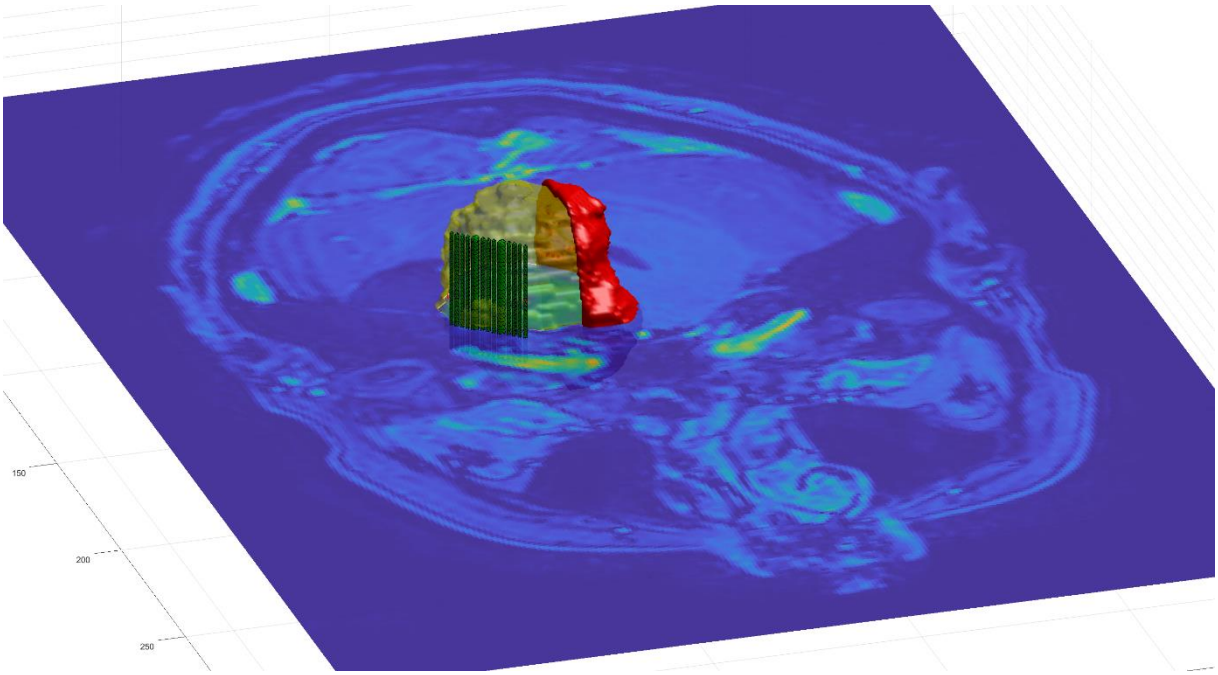

Figure 6: ROI at porus (green square) and between tumor and brainstem (red) visualised together with the tumor (yellow) in an axial slice.

Tractography

ExploreDTI [28] was used to estimate the diffusion tensor and perform the tractography. The software contains an integrated deterministic tractography algorithm [29], which uses ROIs to compute the relevant tracts. The tractography parameters were optimized for facial nerve visualisation in VS patients (Appendix 2). This included the FA threshold, angle threshold and inclusion of a cerebellar exclusion ROI.

The ROI at the brainstem and porus were used as inclusion zones and the cerebellar ROI as an exclusion zone. The parameters in Table 9 were used for all patients.

Table 9: tractography parameters.

Parameter	**Value**
Seedpoint resolution	2 mm isotropic
FA threshold	0.1
Fiber length range	30 – 150 mm
Angle threshold	40 degrees
Step size	1
Interpolation method	linear

Comparison to IO points

The reconstructed tracts were compared against the intraoperative registered points along the course of the facial nerve. For each registered point, the minimal distance to each reconstructed tract within one patient was computed. These distances were averaged over all registered points for each tract. The tract with the lowest average distance to the intraoperative points was defined as the most likely reconstruction of the facial nerve (see Figure 7).

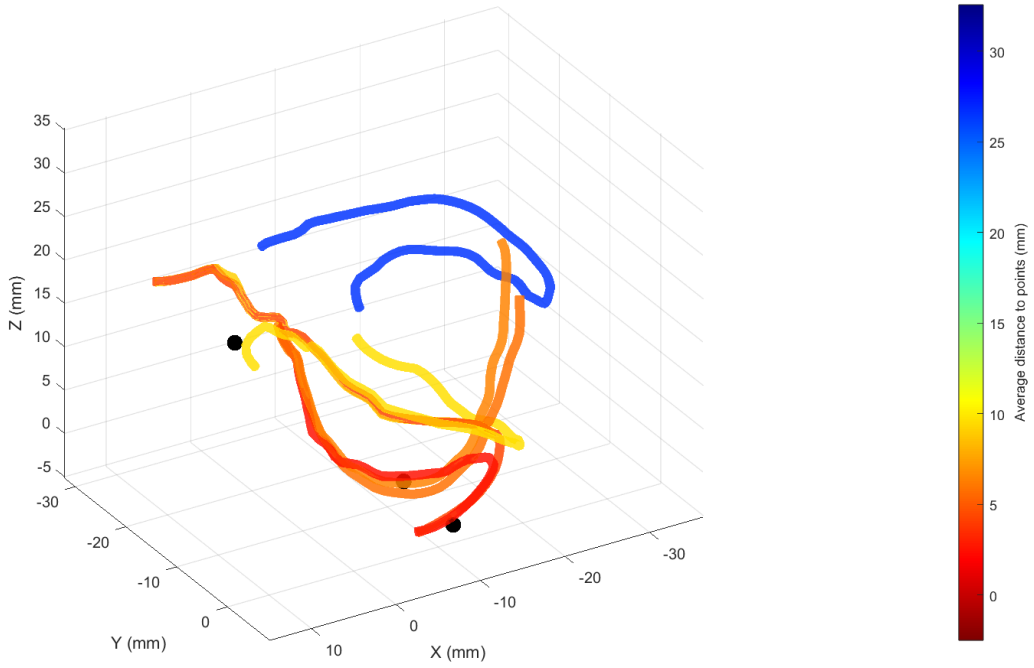

Figure 7: reconstructed tracts and registered points (black) of patient 1. Tracts are coloured based on the average distance to the point, where bright red is the closest.

The points on the best reconstruction that were the closest to the registered points were used for location comparison. The area surrounding the tumor was divided into sextants in the sagittal plane. Point pairs were considered to be 'in agreement' when both points are in the same sextant.

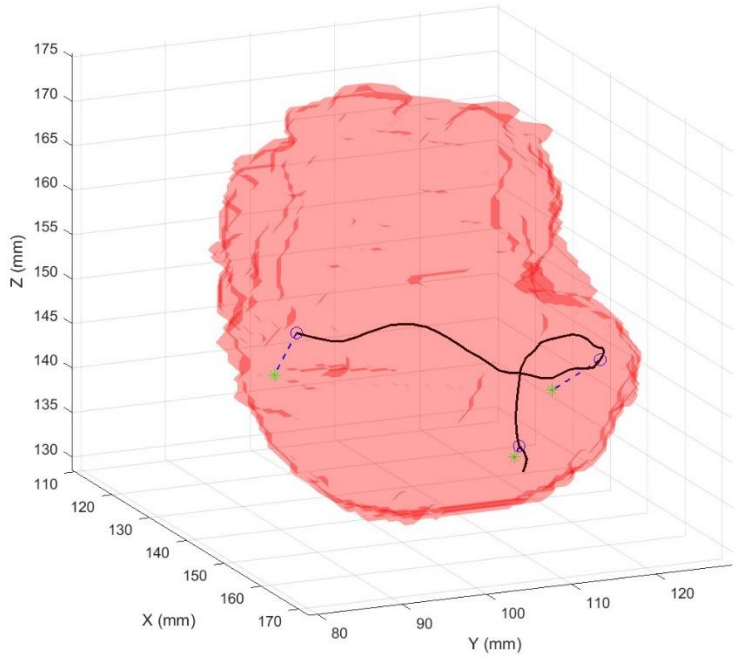

Figure 8: tract points closest to IO points. The green points represent the registered points and the blue point the location on the tract with the shortest distance to the registered point.

Results

Seven patients were included for the validation study. Pathological examination of resected tissues confirmed the diagnosis VS in six out of seven patients, and one patient was diagnosed with a meningioma. This patient was consequently excluded from the study.

All lesions were located on the left side. Tumor diameter varied between 21 and 35 mm. All patient characteristics are summarized in Table 10.

Table 10: patient characteristics.

Patient	Sex	Lesion side	Max tumor diameter (mm)	Remarks
1	Female	Left	34	
2	Female	Left	21	
3	Male	Left	24	
4	Male	Right	11	Excluded
5	Female	Left	29	
6	Female	Left	35	
7	Male	Left	23	

Tract reconstruction was possible in all patients (100%). A total of seventeen control points were registered intraoperatively. Eleven out of seventeen points (65%) were located within the same sextant as the tractography reconstruction. Out of the six remaining points, four were located in an adjacent sextant and two were more than one sextant apart from the tractography reconstructions. When we only consider the first point that was registered in each patient, the agreement increases from 64% to 100% (6/6).

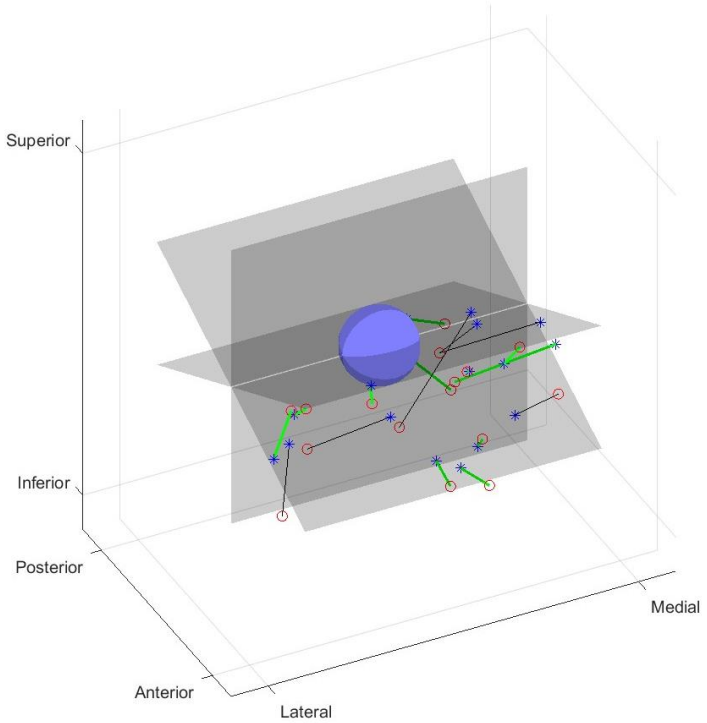

Figure 9: normalised location of nerve according to tractography and registered points. Locations are divided into sextants [10]. Out of seventeen total point pairs, eleven are located in the same sextant (indicated with green lines). Four pairs are in neighbouring sextants and two with a greater distance.

The average distance between the control points and closest tract was 5.5mm (95% CI, 3.6 – 7.4). Points that were not located within the same sextant had an average distance of 8.6mm (95% CI, 5.4 - 11.8) to the tractography reconstructions. This was significantly larger than the 3.7mm (95% CI, 1.8 – 5.7) of the good pairs (ANOVA, F = 10.8, p = 0.005).

Table 11: overview of individual results.

Patient	Tumor type	# registered points	Tracts	Average minimal distance to points (mm)	Agreement (tract and control points)
1	VS	3	Yes	3.73	2/3
2	VS	3	Yes	9.29	1/3
3	VS	3	Yes	1.05	3/3
4	MEN	3	Excluded		
5	VS	3	Yes	7.99	2/3
6	VS	2	Yes	6.48	1/2
7	VS	3	Yes	3.40	2/3

MEN = meningioma

Discussion

In this chapter, we investigated the use of DTI tractography for the preoperative visualisation of the facial nerve. It was possible to reconstruct facial nerve tracts with moderate accuracy. We reconstructed tracts in all patients, which is comparable to recent publications [23], [24].

We used six regions to subdivide the 3D space surrounding the tumor. These sextants represent clinically significant differences in nerve location. 65% of the control points were located within the same sextant as the reconstructed tract. However, there was only one patient where there was agreement between all points and the tract. There was no patient in which there was zero agreement.

The most likely explanation for this result is that the points were registered at different time points during the surgery. The tumor is already partially debulked at the moment of registration of the first point. The first registration was commonly followed by more debulking before the other points were registered. As a result, the anatomical context differed between points. This could cause different shifts of these points relative to one-another, and consequently different agreements. This is confirmed by the fact that the agreement for the points that were registered first in each patient is 100%.

The tumor debulking and resulting shifts are most likely also the main contributor to the distances between the control points and tracts. This distance is on average 5.5mm (95% CI, 3.6 – 7.4), and increases to 8.6mm (95% CI, 5.4 - 11.8) for points and tracts that are not located in the same sextant. This indicates that these mismatches are not accidentally located at the edges between sextans.

Other factor that contribute to the imperfect alignment of control points and tracts are registration and rounding errors within the method and inherent inaccuracies in the

neuronavigation system. We previously investigated errors introduced by the method and found that these are at a sub millimetre level. The target registration error of the neuronavigation system is around the 3mm mark, and only increases as the surgery progresses [31], [32]. This is in line with the average distance of 3.7mm of the correct control points.

Patient 2 and 5 show outliers in the distance measures. The control points registered in these patients were located in unrealistic locations. In both cases, the points were shifted medially, placing them centrally in the brainstem. This was most likely caused by an improper check of the point location during surgery. Despite the shift, the agreement in these patients was comparable to all other patients. This confirms that it was a medial shift, since the shifted points were still in the same sextants as the tracts.

The main limitation of our study was the sample size. We were able to include six patients, five of which were vestibular schwannomas. This was solely due to our short inclusion period. However, we saw a facial nerve location distribution comparable to previous publications in these five patients [10].

We used two different diffusion protocols in our study. This allowed us to start early with the patient inclusion, which was necessary given the low incidence of vestibular schwannomas. The protocols differed in voxel size and the number of diffusion gradients. It is difficult to compare both protocols based on the results of this study since protocol one was only used in two patients of which one had unrealistic control points.

We were one of the first to use intraoperatively registered control points as comparison for tractography. Where previous publications reduce the facial nerve location to one 2-dimensional descriptor [10], we were able to compare tracts and control points in 3D. The use of registered points helps with outcome standardisation, which is suggested to be necessary before clinical implementation [9], [14]. It is important to consider that this method also introduces its own errors, which were previously discussed.

Our tractography results contained false positives in each patient. We expect that the use of more (specific) ROIs can help to reduce the number of false positives. A large number of false positives could be identified by their unrealistic trajectory, e.g. a tract which was coiled in the centre of the tumor. Exclusion ROIs and more precise seed ROI placement could help with the removal of these tracts. However, it is important to consider that the inclusion of more (manually) placed ROIs is also bias sensitive [14].

We used the location of the intraoperative points to retrospectively filter out the best tract. In a preoperative setting, we would rely on the judgement of the surgeon to select the tract that most likely resembles the facial nerve. A clinical feasibility study could give insight in the performance of the current method, and which visualisation method is most suitable for clinical implementation.

Conclusion

DTI-based tractography can be used to preoperatively visualise the facial nerve in patients with vestibular schwannomas. Reconstructions largely fall within clinically acceptable ranges, but can be further improved. The next step should be to reduce the number of false-positive tracts to improve the ambiguity and thus clinical usability.

CHAPTER 3

Preoperative visualisation of facial nerve tractography in patients with cerebellopontine angle tumors using AR

Introduction

DTI-based tractography is a promising method for facial nerve visualization in patients with vestibular schwannoma's [9], [26]. However, previous research shows that it requires experienced operators and that its clinical reproducibility is limited, mainly due to the heterogeneity of the methods that are used. As a result, no large clinical studies investigating the clinical benefit of visualizing the facial nerve with DTI have been performed.

An important factor to improve reproducibility and clinical applicability is data presentation to clinicians. It is increasingly common to create 3D representations of the nerve tracts in combination with the original T1 scan and/or a 3D segmentation of the tumor and present it on a regular 2D screen. An upcoming visualization technique for surgical planning is augmented reality (AR). Recent years have shown an increase in research on the implementation of AR in the department of neurosurgery. The research mainly focuses on the use of AR for neuronavigation, but also includes assessment of AR for resident training, medical education and patient information purposes [33], [34], [35], [36].

In patients with vestibular schwannoma's, AR has been used to visualize segmented structures such as the tumor, trigeminal nerve and transverse and sigmoid sinus. These structures were superimposed onto the surgical field using the surgical microscope. This reportedly improved orientation in the operative field, but did not lead to significant differences in clinical outcome or complication rates [37].

We expect 3D visualisations in AR to aid in the interpretation of facial nerve tractography and the localization of the facial nerve. Consequently, this could potentially lead to an improvement in clinical outcome after surgical resection of the schwannoma. This study is the first step towards evaluating the clinical use of tractography visualisation in AR.

Objective: to evaluate the value of preoperative facial nerve tractography visualised using AR in patients with cerebellopontine angle tumors.

Method

Patient that were treated in the UMC Utrecht for the surgical resection of pontine angle tumors were included in this study. All patients received the standard pre-operative imaging, consisting of a T1c scan, in addition to a dMRI scan. The T1c scan was uploaded to the Lumi (Augmedit B.V., Naarden, the Netherlands) environment. The integrated segmentation tools were used to make 3D models of the brain, skin and tumor [30].

All diffusion data was uploaded to ExploreDTI [28]. An integrated deterministic tractography algorithm [29] was used to reconstruct the course of the facial nerve near the tumor (as specified in Chapter 2). The reconstructed tracts were exported as 3D tubes and uploaded to the Lumi. The T1c scan, segmented structures and tractography results were all converted into a stereoscopic image which was visualised using the HoloLens 2 (Microsoft, Redmond, USA).

Before surgery, the neurosurgeon was presented with the stereoscopic image, in the same orientation as the patient's head during surgery. The surgeon could freely adjust the visibility of all the structures. There was no time limit for the examination of the stereoscopic image. After the examination, the surgeon was asked what the expected location of the facial nerve was, based on the stereoscopic image. At the end, the surgeon was asked to manually register it to the patient.

During surgery, the BrainLab neuronavigation system was used and registered to the T1c scan. The surgeon was asked to register at least 3 points along the trajectory of the facial nerve using the neuronavigation tools. This was done either after visual localisation of the facial nerve or localisation using neurostimulation. These points should be located at the brainstem, at the porus and halfway down the nerve. Additionally, images were taken using the microscope. This was done when the facial nerve was visible in the surgical field.

The surgeon scored to what extent the tractography results corresponded with the intraoperative location of the facial nerve on a five-point Likert scale, where '1' indicates 'Strongly Disagree' and '5' indicates 'Strongly Agree'. Additionally, the tract locations were compared against the intraoperatively registered points to validate the surgeons score.

After surgery, the surgeon was asked to fill out a questionnaire (Appendix 3). The results of all cases were combined and grouped into Agreement, Method, Visualisation and Future perspectives (Table 12). Descriptive statistics, consisting of the median and interquartile range (IQR) were computed for both the method and visualisation groups. Additional comments were reported separately.

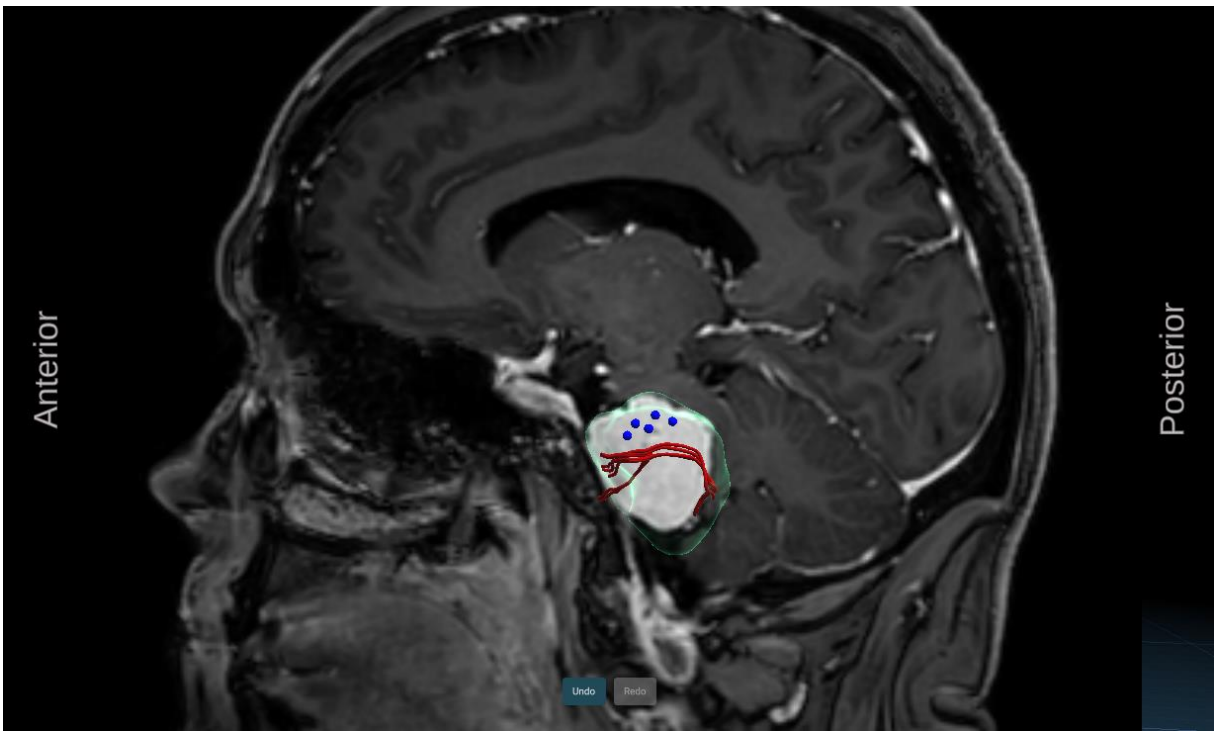

Figure 10: Case 1. Visualisation of tumor (transparent green), tractography results (red) and control points (blue) in a sagittal plane.

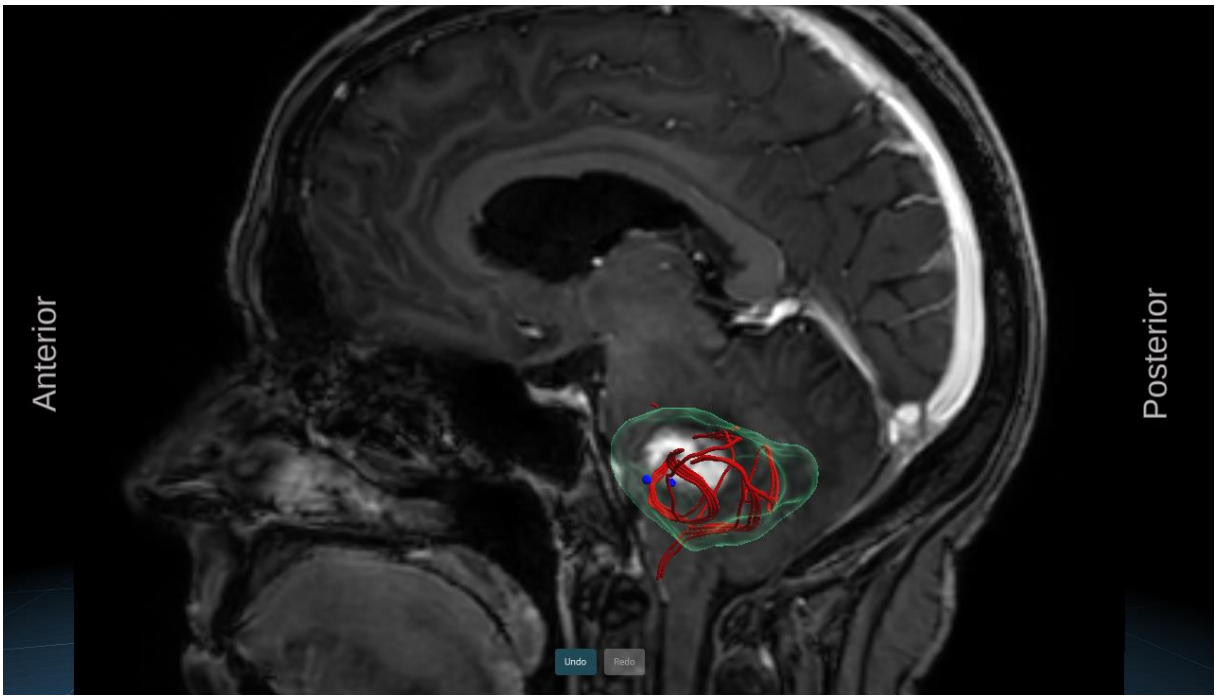

Figure 11: Case 2. Visualisation of tumor (transparent green), tractography results (red) and control points (blue) in a sagittal plane.

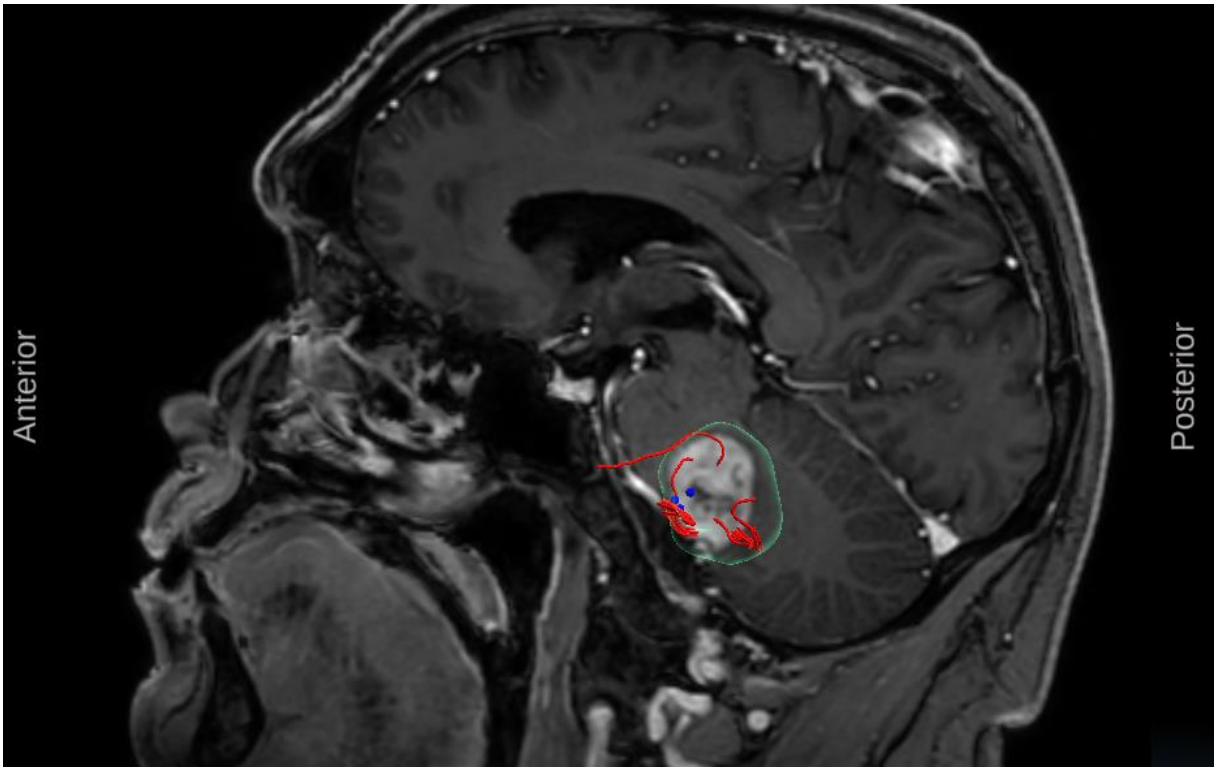

Figure 12: Case 3. Visualisation of tumor (transparent green), tractography results (red) and control points (blue) in a sagittal plane.

Results

Three patients, treated by two different neurosurgeons, were included in this study. One was diagnosed with a meningioma, and the other two with a vestibular schwannoma. We were able to reconstruct the facial nerve using tractography and visualised it with AR in all patients. All reconstructions could be made within four hours, making it possible to integrate the method in the standard clinical workflow.

Intraoperative point registration along the facial nerve trajectory was possible in all patients . Five points were registered in the first case (Figure 10), two in the second (Figure 11) and three in the third case (Figure 12). In all cases, the points were located in realistic positions.

The tract reconstructions contained multiple fibers, leaving it up to the surgeon to choose the tract which most likely represented the facial nerve. For case one, the surgeon estimated the tract to curve around the posterior side of the tumor based on the tractography results (Figure 10). In case two, the nerve location was estimated to be anterior to the tumor based on the tractography results (Figure 11). This was similar to the third case (Figure 12).

Both surgeons filled out the questionnaire after the surgeries (Table 12). The agreement with the intraoperative location was scored 3 out of 5 in the first two cases, and 4 out of 5 in the third case. The results for questions in the categories “Method’ and ‘Visualisation’ are visualised in box plots (Figure 13). Both surgeons were moderately positive about the method (median 4, IQR 3.5 - 4) and visualisation (median 4, IQR 3.5 – 4.25).

Table 12: questionnaire results.

Agreement	**Case 1**	**Case 2**	**Case 3**
The facial nerve location in the 3D model corresponds to the intraoperative location	3	3	4
The method changed my expectation of the facial nerve location	4	1	4
The method is beneficial form my understanding of the expected intraoperative facial nerve location	4	2	5
The method is beneficial for the treatment of patients	4	3	4
The method is useful in the preoperative setting	4	4	4
This method can make the surgery faster	4	2	4
It was easy to translate the information from the imaging to the intraoperative setting	4	2	4
It is necessary to register the stereoscopic image onto the patient to fully exploit the benefits of the preoperative facial nerve localization	4	1	4
The visualisation method is important for my understanding of the data	5	5	4
I think that further improvements are necessary before clinical implementation	4	5	4
Additional comments			
The tractography estimation seems to be inferior to the real location in case 1			
The false positives make it difficult to interpret the data			
It would be nice to mark the origin of the facial nerve on the brainstem			

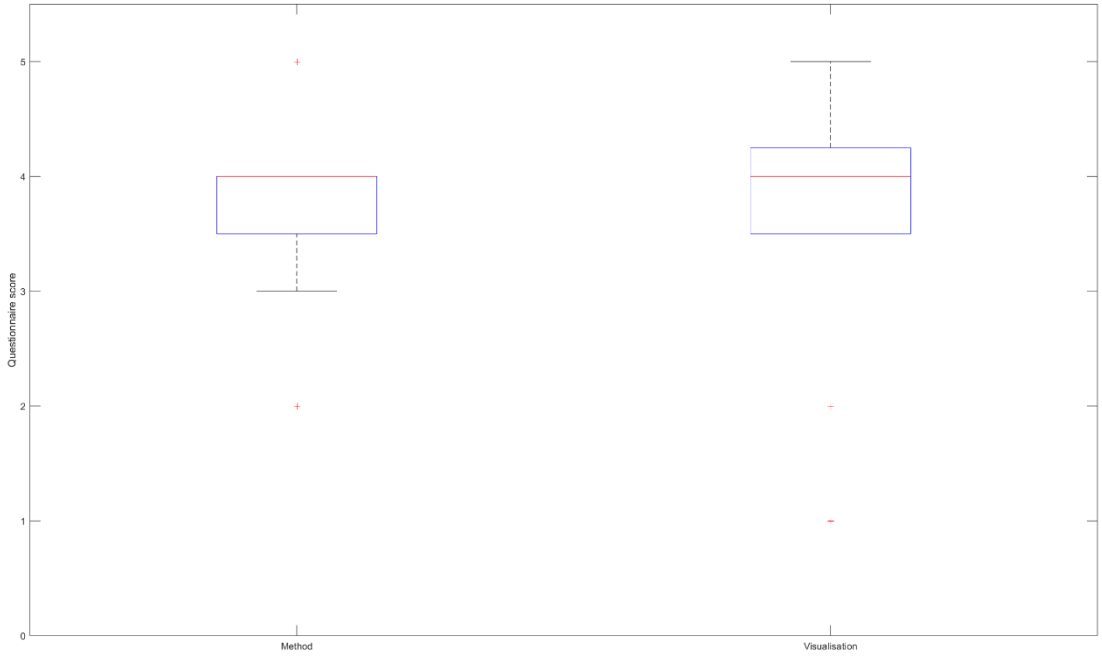

Figure 13: Boxplot of grouped questionnaire results. The red line represents the median value, the surrounding box the interquartile range. The whiskers show the minimum and maximum values. Red crosses are outlier values.

Discussion

We were one of the first to use AR to visualize facial nerve tractography results in patients with cerebellopontine angle tumors. The initial experience of the surgeons was positive, as indicated by the questionnaire. Both surgeons acknowledged the potential of the method and experienced the AR visualisation as beneficial for their spatial understanding and interpretation of the tractography results.

We were able to use the neuronavigation system to register points in both patients. However, in one patient we were only able to register two points. In this patient, the neurostimulator had to be used to localise the facial nerve. It was not possible to localise the nerve in more the two locations, resulting less control points. However, this did not negatively affect the results of this study.

The agreement between the tractography results and intraoperative nerve location was scored 3 – 4 out of 5 by both surgeons. In case one, the surgeon specifically mentioned that the tractography results were inferior to the true location. This was consistent with the location of the registered points. The tracts and points were also relatively close together in case two, indicating that the surgeons were able to correctly translate the tractography results to the intraoperative setting. This was confirmed by the questionnaire results.

Disagreements between surgeons were most likely due to the case-specific tractography results. The results were more inconclusive in case 2 because of a larger amount of false-positive tracts. This is reflected in the lower scores across the questionnaire for case 2. Combined with the surgeon's comments, this underlines the importance of false-positive reduction before the clinical usefulness of the method can be properly evaluated.

Conclusion

Augmented reality has the potential to improve the spatial understanding and interpretation of tractography results in patients with cerebellopontine tumors. However, false-positive tracts hinder the usefulness and evaluation of the method. Prior to clinical implementation studies, future research should focus on improving the precision of the tractography results, and making it less prone to false-positive results.

General discussion

We were able to investigate facial nerve tractography from scan protocol selection until data presentation in a clinical setting. Our work was subdivided into three chapters, discussing the initial feasibility of facial nerve tractography in healthy nerves, the use of the method in patients with vestibular schwannomas and the clinical visualization and usability of this data.

In the first chapter, we found that it was possible to reconstruct facial nerve trajectories using the clinical protocol diffusion MRI scans. Tract reconstruction quality using the clinical protocol was not optimal. We investigated the reconstruction errors and found that the scan quality was a limiting factor for the reconstruction quality. Alternatively, we also concluded that errors introduced by the data processing method were not big enough to be of clinical significance. These findings were instrumental for the scan protocol selection and method selection in the subsequent chapters.

The second chapter investigated the use of facial nerve tractography in patients with vestibular schwannomas. Reconstructions could be made in all patients, albeit with a high false-positive rate. The comparison with intraoperatively registered points along the facial nerve trajectory allowed for quantitative metrics, which is a first in this field. However, tissue shifts during surgery negatively influenced these comparisons. We concluded that method improvements should initially be focussed on false-positive rate reduction before clinical validation can take place. However, we also suggested that a clinical feasibility study could give more insight into the clinical endpoints of such improvements.

In the third chapter, we investigated the clinical feasibility of using AR to visualize tractography results in patients with cerebellopontine angle tumors. Although reconstructions could be made in all patients, it was difficult for the surgeon to identify the tract representative of the facial nerve because of the false positives. Once identified, the visualisation method was very useful in translating the tract location to the intraoperative setting. This underlines the potential of AR to improve spatial understanding of the data in anatomically complex locations, potentially reducing observer-variation.

Thus far, tractography results have always been highly operator dependent [9], [24]. This is mostly because of the manual ROI placement. In this study, we were able to place two out of three ROIs automatically. The addition of automatic porus detection would allow us automate the entire ROI placement process, reducing operator dependencies and improving consistency. This could potentially be done using deep learning approaches, which would not require additional scans to be made.

Our study again underlines the benefit of AR in visualisation of 3D structures. It lends itself for the complex location of vestibular schwannomas, and the translation of preoperative imaging to an intraoperative setting [36]. Other visualisation methods such as a regular 2D viewer and 3D models on a 2D screen were considered. We expected that these methods would introduce observer-variation, especially when the surgeon determines the agreement between the tractography and intraoperative setting. AR most likely minimized this variation, which was of importance because of the low number of included patients [36].

The strength of this report is that it encompasses the entire clinical workflow of facial nerve tractography, which is very rare in this field [9]. This allows us to evaluate our method in a clinical context. The main outcome is that in order for the method to be useful, the number of false positives should be reduced. This allows for a better understanding and interpretation of the tractography results by clinicians.

Limitations

Small sample sizes were limiting factors in both the second and third chapter. The prospective nature of these parts, combined with the low incidence of vestibular schwannomas, severely limited the amount of patients that could be included. Clinical implementation of tractography would require a large-scale clinical validation study. The data results we gathered is an initial step toward this goal.

One of the downsides of the methods used in this research, is that it relies on a lot of different software packages. The increases the possibility of operator error when reconstructing the tracts, but also mean that it takes more time to generate the tracts. An initial step could be to combine the steps in ExploreDTI with those in MATLAB since both are based on MATLAB libraries. We expect that this would significantly cut down the preparation time of the tracts.

Tractography relies on modelling and assumptions. Reconstructed tracts are only related to the nerve trajectories in an indirect manner. This is why interpretation might not be as straightforward as it seems. This is especially true in regions with crossing white-matter tracts. Consequently, surgeons should have a basic understanding of the methodology behind tractography, and more specifically its limitations and accuracy [14]. We did not test the surgeons understanding of tractography, and relied on the researcher to put the results in context.

Future perspectives

Our recommendation would be to continue the inclusion of patients with vestibular schwannomas using the dMRI protocol we proposed in this study. This would only require one additional scan to be made prior to surgery and the registration of points during surgery. It would be worth-while to reconsider the timing of the point registration to minimize changes in anatomical shifts between points, maximizing the added benefit of the quantitative comparison metrics.

In the meantime, we would suggest method updates consisting of ROI optimisation to reduce false-positive rates and the integration of all steps into one software package to minimize the chances of errors. Alternative tractography algorithms could be investigated. Based on literature, however, we would not expect these to improve the performance of facial nerve tractography while it does make the method and interpretation more complex.

Conclusion

We investigated the entire workflow surrounding facial nerve tractography in patients with vestibular schwannomas. Our work consists of dMRI protocol selection, tractography methodology as well as clinical presentation of the results using AR. We were able to reconstruct the facial nerve tracts and evaluate the accuracy of these reconstructions intraoperatively using quantitative metrics. We set the first steps towards method standardisation by including automatic ROI selection as well as a less observer-variant visualisation method. Our findings suggest that the false positive rate is currently the biggest hurdle to overcome before clinical use of the method. Continuing and improving upon this work would allow for tractography standardisation, and consequently proper evaluation. This would bring facial nerve tractography closes to clinical implementation.

References

[1] M. L. Carlson and M. J. Link, "Vestibular Schwannomas," *New England Journal of Medicine*, vol. 384, no. 14, pp. 1335–1348, Apr. 2021, doi: 10.1056/NEJMra2020394.

[2] V. K. Gupta, A. Thakker, and K. K. Gupta, "Vestibular Schwannoma: What We Know and Where We are Heading," Dec. 01, 2020, *Springer*. doi: 10.1007/s12105-020-01155-x.

[3] R. Goldbrunner *et al.*, "Eano guideline on the diagnosis and treatment of vestibular schwannoma," *Neuro Oncol*, vol. 22, no. 1, pp. 31–45, Jan. 2020, doi: 10.1093/neuonc/noz153.

[4] W. T. Koos, R. F. Spetzler, and J. Lang, *Color Atlas of Microneurosurgery*, vol. 1. 2013.

[5] Y. Zhang *et al.*, "Facial nerve preservation with preoperative identification and intraoperative monitoring in large vestibular schwannoma surgery," *Acta Neurochir (Wien)*, vol. 155, no. 10, pp. 1857–1862, Oct. 2013, doi: 10.1007/s00701-013-1815-9.

[6] S. F. Ansari, C. Terry, and A. A. Cohen-Gadol, "Surgery for vestibular schwannomas: A systematic review of complications by approach," *Neurosurg Focus*, vol. 33, no. 3, Sep. 2012, doi: 10.3171/2012.6.FOCUS12163.

[7] J. W. House and D. E. Brackmann, "Facial nerve grading system."

[8] A. R. Savardekar *et al.*, "Preoperative diffusion tensor imaging-fiber tracking for facial nerve identification in vestibular schwannoma: A systematic review on its evolution and current status with a pooled data analysis of surgical concordance rates," *Neurosurg Focus*, vol. 44, no. 3, Mar. 2018, doi: 10.3171/2017.12.FOCUS17672.

[9] A. Bubeníková, A. Vlasák, Z. Fík, V. Sedlák, M. Tesařová, and O. Bradáč, "Application of diffusion tensor imaging of the facial nerve in preoperative planning for large vestibular schwannoma: a systematic review," *Neurosurg Rev*, vol. 46, no. 1, Dec. 2023, doi: 10.1007/s10143-023-02214-x.

[10] P. Sampath, D. Rini, and D. M. Long, "Microanatomical variations in the cerebellopontine angle associated with vestibular schwannomas (acoustic neuromas): a retrospective study of 1006 consecutive cases," *J Neurosurg*, vol. 92, no. 1, pp. 70–78, Jan. 2000, doi: 10.3171/jns.2000.92.1.0070.

[11] L. Yao, B. Wang, F. Lu, X. He, G. Lu, and S. Zhang, "Facial nerve in skullbase tumors: imaging and clinical relevance," Dec. 01, 2023, *BioMed Central Ltd*. doi: 10.1186/s40001-023-01078-7.

[12] E. O. Stejskal and J. E. Tanner, "Spin diffusion measurements: Spin echoes in the presence of a time-dependent field gradient," *J Chem Phys*, vol. 42, no. 1, pp. 288–292, 1965, doi: 10.1063/1.1695690.

[13] J. M. Soares, P. Marques, V. Alves, and N. Sousa, "A hitchhiker's guide to diffusion tensor imaging," *Front Neurosci*, no. 7 MAR, 2013, doi: 10.3389/fnins.2013.00031.

[14] B. Jeurissen, M. Descoteaux, S. Mori, and A. Leemans, "Diffusion MRI fiber tractography of the brain," Apr. 01, 2019, *John Wiley and Sons Ltd*. doi: 10.1002/nbm.3785.

[15] T. Taoka *et al.*, "Displacement of the facial nerve course by vestibular schwannoma: Preoperative visualization using diffusion tensor tractography," *Journal of Magnetic Resonance Imaging*, vol. 24, no. 5, pp. 1005–1010, Nov. 2006, doi: 10.1002/jmri.20725.

[16] V. M. Gerganov, M. Giordano, M. Samii, and A. Samii, "Diffusion tensor imaging-based fiber tracking for prediction of the position of the facial nerve in relation to large vestibular schwannomas: Clinical article," *J Neurosurg*, vol. 115, no. 6, pp. 1087–1093, Dec. 2011, doi: 10.3171/2011.7.JNS11495.

[17] P. H. Wei *et al.*, "Identification of cranial nerves near large vestibular schwannomas using superselective diffusion tensor tractography: experience with 23 cases," *Acta Neurochir (Wien)*, vol. 157, no. 7, pp. 1239–1249, Jul. 2015, doi: 10.1007/s00701-015-2431-7.

[18] S. A. Borkar *et al.*, "Prediction of facial nerve position in large vestibular schwannomas using diffusion tensor imaging tractography and its intraoperative correlation," *Neurol India*, vol. 64, no. 5, pp. 965–970, Sep. 2016, doi: 10.4103/0028-3886.190270.

[19] F. Song *et al.*, "In vivo visualization of the facial nerve in patients with acoustic neuroma using diffusion tensor imaging-based fiber tracking," *J Neurosurg*, vol. 125, no. 4, pp. 787–794, Oct. 2016, doi: 10.3171/2015.7.JNS142922.

[20] O. Hilly *et al.*, "Diffusion Tensor Imaging Tractography of the Facial Nerve in Patients With Cerebellopontine Angle Tumors," 2016.

[21] H. Li *et al.*, "Identification of the Facial Nerve in Relation to Vestibular Schwannoma Using Preoperative Diffusion Tensor Tractography and Intraoperative Tractography-Integrated Neuronavigation System," *World Neurosurg*, vol. 107, pp. 669–677, Nov. 2017, doi: 10.1016/j.wneu.2017.08.048.

[22] Y. Zhang *et al.*, "Preoperative Prediction of Location and Shape of Facial Nerve in Patients with Large Vestibular Schwannomas Using Diffusion Tensor Imaging–Based Fiber Tracking," *World Neurosurg*, vol. 99, pp. 70–78, Mar. 2017, doi: 10.1016/j.wneu.2016.11.110.

[23] Y. Zhang, H. Ge, M. Xu, and W. Mei, "Significance of Preoperative Nerve Reconstruction Using Diffusion Tensor Imaging Tractography for Facial Nerve Protection in Vestibular Schwannoma," *J Korean Neurosurg Soc*, vol. 66, no. 2, pp. 183–189, Mar. 2023, doi: 10.3340/jkns.2022.0134.

[24] T. Szmuda *et al.*, "Reliability of diffusion tensor tractography of facial nerve in cerebello-pontine angle tumors," *Neurol Neurochir Pol*, vol. 54, no. 1, pp. 73–82, 2020, doi: 10.5603/PJNNS.a2020.0001.

[25] A. Fedorov *et al.*, "3D Slicer as an image computing platform for the Quantitative Imaging Network," *Magn Reson Imaging*, vol. 30, no. 9, pp. 1323–1341, Nov. 2012, doi: 10.1016/j.mri.2012.05.001.

[26] V. Baro *et al.*, "Preoperative Prediction of Facial Nerve in Patients with Vestibular Schwannomas: The Role of Diffusion Tensor Imaging—A Systematic Review," May 01, 2019, *Elsevier Inc.* doi: 10.1016/j.wneu.2019.01.099.

[27] S. Klein, M. Staring, K. Murphy, M. A. Viergever, and J. P. W. Pluim, “Elastix: A toolbox for intensity-based medical image registration,” *IEEE Trans Med Imaging*, vol. 29, no. 1, pp. 196–205, Jan. 2010, doi: 10.1109/TMI.2009.2035616.

[28] A. Leemans, B. Jeurissen, J. Sijbers, and D. K. Jones, “ExploreDTI: a graphical toolbox for processing, analyzing, and visualizing diffusion MR data,” 2009. [Online]. Available: http://www.ExploreDTI.com.

[29] P. J. Basser, S. Pajevic, C. Pierpaoli, J. Duda, and A. Aldroubi, “In vivo fiber tractography using DT-MRI data,” *Magn Reson Med*, vol. 44, no. 4, pp. 625–632, 2000, doi: 10.1002/1522-2594(200010)44:4<625::AID-MRM17>3.0.CO;2-O.

[30] T. Fick *et al.*, “Fully automatic brain tumor segmentation for 3D evaluation in augmented reality,” *Neurosurg Focus*, vol. 51, no. 2, pp. 1–8, Aug. 2021, doi: 10.3171/2021.5.FOCUS21200.

[31] M. N. Wang and Z. J. Song, “Classification and analysis of the errors in neuronavigation,” Apr. 2011. doi: 10.1227/NEU.0b013e318209cc45.

[32] L. H. Stieglitz *et al.*, “The silent loss of neuronavigation accuracy: A systematic retrospective analysis of factors influencing the mismatch of frameless stereotactic systems in cranial neurosurgery,” *Neurosurgery*, vol. 72, no. 5, pp. 796–807, May 2013, doi: 10.1227/NEU.0b013e318287072d.

[33] R. Mishra, K. Narayanan, G. E. Umana, N. Montemurro, B. Chaurasia, and H. Deora, “Virtual Reality in Neurosurgery: Beyond Neurosurgical Planning,” Feb. 01, 2022, *MDPI*. doi: 10.3390/ijerph19031719.

[34] T. M. Kos, E. Colombo, L. W. Bartels, P. A. Robe, and T. P. C. van Doormaal, “Evaluation Metrics for Augmented Reality in Neurosurgical Preoperative Planning, Surgical Navigation, and Surgical Treatment Guidance: A Systematic Review,” *Operative Neurosurgery*, Dec. 2023, doi: 10.1227/ons.0000000000001009.

[35] E. Colombo *et al.*, “Mixed Reality for Cranial Neurosurgical Planning: A Single-Center Applicability Study With the First 107 Subsequent Holograms,” *Operative Neurosurgery*, Dec. 2023, doi: 10.1227/ons.0000000000001033.

[36] T. Fick, J. W. Meulstee, M. H. Köllen, J. A. M. Van Doormaal, T. P. C. Van Doormaal, and E. W. Hoving, “Comparing the influence of mixed reality, a 3D viewer, and MRI on the spatial understanding of brain tumors,” *Front Virtual Real*, vol. 4, 2023, doi: 10.3389/frvir.2023.1214520.

[37] M. Pojskić, M. H. A. Bopp, B. Saß, and C. Nimsky, “Single-Center Experience in Microsurgical Resection of Acoustic Neurinomas and the Benefit of Microscope-Based Augmented Reality,” *Medicina (Lithuania)*, vol. 60, no. 6, Jun. 2024, doi: 10.3390/medicina60060932.

[38] J. Y. M. Yang, C. H. Yeh, C. Poupon, and F. Calamante, “Diffusion MRI tractography for neurosurgery: The basics, current state, technical reliability and challenges,” Aug. 07, 2021, *IOP Publishing Ltd*. doi: 10.1088/1361-6560/ac0d90.

Appendix

1. Diffusion protocol selection

The diffusion protocol selection for Chapter 2 of our study was based on multiple factors. We concluded in Chapter 1 that the clinically used diffusion protocol is not sufficient for facial nerve tractography purposes in patients with VSs. In this section, we combine our findings from Chapter 1 with an additional literature search, practical considerations and expert opinion to define the required diffusion scan parameters for facial nerve tractography in patients with VSs.

Literature search

Over the past two decades, a lot of different diffusion protocols have been used for facial nerve tractography (Table 13). The largest voxel size reported is 2 mm^3, and the number of diffusion gradients vary from 12 to 64. However, the b-value for the gradients is consistent across studies. All but one study used 1000 s/mm^2.

Table 13: overview of acquisition parameters used in literature

Study	Voxel size [mm]	Slice thickness [mm]	Diffusion gradients	b-value [s/mm^2]	Success (%)	Agreement (%)
Taoka, 2006 [15]	1.8 x 1.8	1	Unclear	1000	7/8	5/7
Gerganov, 2011 [16]	Unclear	1.6	12	1000	22/22	20/22
Zhang, 2013 [5]	1.8 x 1.8	3	Unclear	1000	7/8	7/7
Wei, 2015 [17]	Unclear	2	30	NA		
Borkar, 2016 [18]	0.78 x 0.78 (reconstructed)	1.5	15	800	19/20	16/18
Song, 2016 [19]	1.6 x 1.6	1.2	30	1000	14/15	13/14
Hilly, 2016 [20]	2 x 2	2	32	Unclear	20/21	15/21
Li, 2017 [21]	1.8 x 1.8	1	32	1000	18/19	17/18
Zhang, 2017 [22]	Unclear	2	64	1000	30/30	29/30
Szmuda, 2020 [24]	1.5 x 1.5	1.5	20	1000	35/38	31/35
Zhang, 2023 [23]	Unclear	1	30	1000	27/30	25/27

In these studies, the success rate is defined as the percentage of patients where a tract could be reconstructed. It ranges from 88% to 100%. The agreement is the percentage of patients in which the tract corresponded with the location of the facial nerve, which ranges from 71% to 100%. However, it is important to note that the number of patients included was low in all studies, with a maximum of 35.

We plotted the different scan parameters against the success and agreement percentages to identify potential correlations (Figure 14). However, no obvious correlations were found.

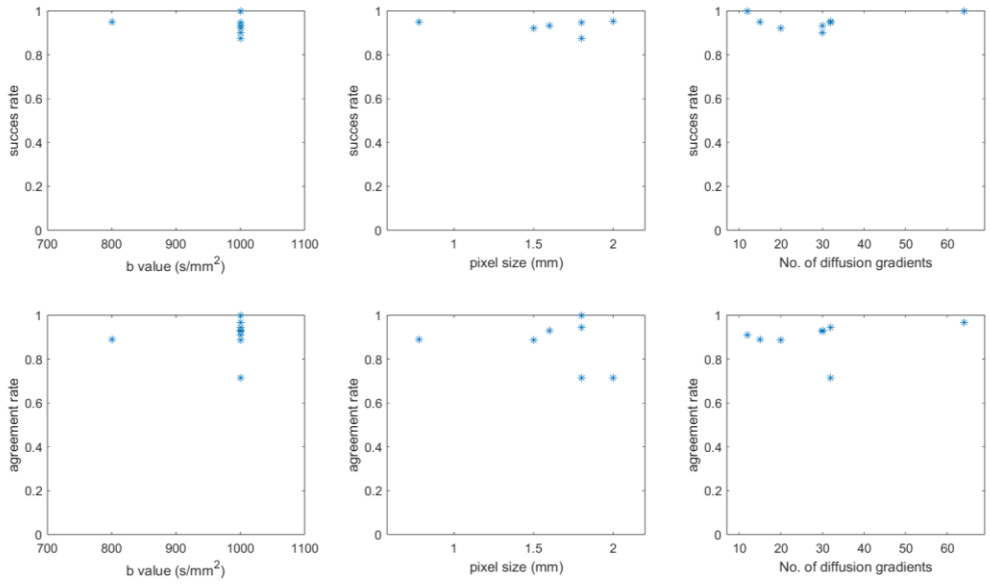

Figure 14: different diffusion scan parameters plotted against the success and agreement rates as reported in literature.

Based on the results in literature, we concluded that the isotropic voxel size should be at maximum 2mm, that the minimum amount of diffusion gradients is 30 and the b-value needs to be 1000 s/mm^2.

Practical considerations

Practical considerations need to be taken into account since the protocol will be part of the presurgical workflow of the patients. The most important restriction is the scan time. A maximum of 10 additional minutes are allowed to be added to the regular scan time. This included aligning the patient and preparing the sequence. A smaller voxel size and increase in the amount of diffusion directions scale linearly with the scan time.

The signal-to-noise ratio decreases for smaller voxel sizes and lower MRI field strengths. A 3T MRI scanner was available to scan our patients. As a result, the signal-to-noise ratio (SNR) would most likely be bad when scanning voxels sizes smaller than 2mm isotropic. This could be counteracted by averaging over more excitations, but this also increases scan time. For example, averaging over two excitations instead of one doubles the scan time.

Expert opinion

Prof. A. Leemans (Image Sciences Institute, UMC Utrecht, the Netherlands) was consulted for the development of the diffusion sequence. He advised on which parameter adaptations would most likely result in the best quality improvement given the constraints. He specifically advised on the balance between voxel size, SNR and scan time. A voxel size of 2 mm isotropic was deemed sufficient without averaging over multiple acquisitions. However, he advised to prioritise voxel size in case there was room to increase the scan duration.

Conclusion

We defined our scan parameters based on our findings in Chapter 1, the literature search, practical considerations and expert input. They are summarized in Table 14. The scan duration of 392 seconds (~6.5 minutes) fit exactly in the 10 minute requirement of the radiology department when also accounting for the preparation duration. As a result, there was no more room for further improvements in the protocol.

Table 14: summary of diffusion scan parameters.

Parameter	**Value**
Voxel size	2 x 2 x 2 mm
Slice thickness	2 mm
Number of diffusion gradients	32
b-value	1000 s/mm^2
Echo time	92 ms
Repetition time	10318 ms
Number of averages	1
Scan time	329 s

2. Tractography parameter optimisation

Multiple tractography parameters can be adjusted to make the reconstructed tracts more/less specific. This includes seed point resolution, FA threshold, angle threshold, interpolation method and interpolation step size. Out of these, the FA and angle threshold are varied most often [9].

These termination criteria respectively indicate at which FA value and which angle the algorithm stops tracking the reconstructed tract. Lower FA values and larger angles will result in a more sensitive algorithm, and consequently more false positives. Alternatively, high FA thresholds and small angles will generate more specific results.

We investigated different combinations of FA and angle threshold to find the optimal combination for facial nerve tractography in patients with vestibular schwannomas. The focus is to find the combination that includes the least amount of false positives (reconstructed tracts that do not represent the facial nerve), whilst generating results in all patients.

Methods

We used the data of the first five patients included in the study reported in Chapter 2 to reconstruct tracts using different combinations of FA and angle thresholds. We used the same tractography methodology as reported in that chapter.

For the first patient, we used FA values of 0.05, 0.10 and 0.15 and angles of 30, 45, 70 and 90 degrees (Figure 15). Based on these initial results, we further specified the parameter combinations. We narrowed these down to an FA value of 0.1 and angles of 30, 35, 40 and 45 degrees. We used these parameters to reconstruct tracts in all five patients. Based on these results, we select the parameter combinations which gives results in the most amount of patients while being as specific as possible.

Next, we investigate the benefit of using the cerebellum as an exclusion ROI. We used the best parameters from the previous step and used them to compute tracts with and without the usage of the cerebellar ROI. In the comparison, we looked if the additional ROI reduced the number of false positives without affecting the potential realistic tracts.

For each patient, we checked if it was possible to reconstruct tracts using the different parameter combinations. The reconstructed tracts were visually inspected for location and trajectory likeliness.

Results

The result in the first patient are summarised in Figure 15. Tracts were reconstructed for FA values equal to or lower than 0.1, and angles equal to or greater than 45 degrees. Lower FA thresholds and larger angles resulted in more reconstructed tracts. There were still many different trajectories present in all parameter combinations. The parameter combinations were therefore changed to an FA value of 0.1 and angles of 30, 35, 40 and 45 degrees.

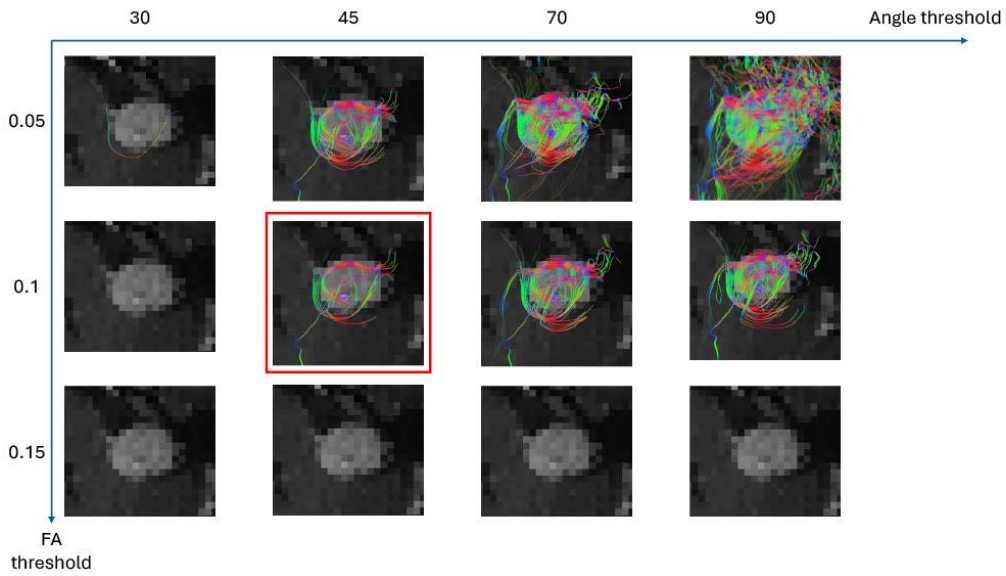

Figure 15: overview of tractography results for different FA and angle thresholds. The orange box surrounds the parameter combination with the best results.

Figure 16 illustrates the results for all patients using the different combinations of FA and angle thresholds. Reconstructions could be made in four out of five patients using all combinations except one. One patient, P4, did not generate results using any of the combinations used, also including the previous parameter combinations.

Visual inspection concluded that all combinations resulted in reconstructed tracts that were likely to represent the facial nerve. Stricter thresholds, e.g. lower angels and higher FA values, reduced the amount of false positives in all patients.

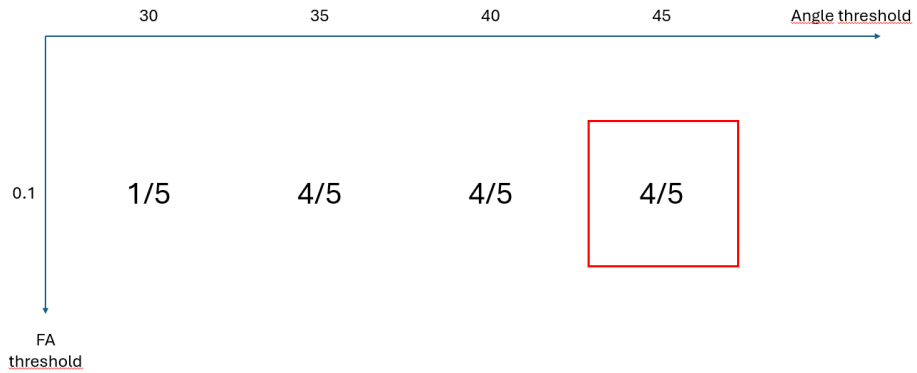

Figure 16: overview of amount of patients in which tracts could be reconstructed using different combinations of FA and angle thresholds. The orange box corresponds to the one depicted in Figure 15.

The results with and without the cerebellar ROI are visualised in Figure 17. The addition of the ROI filters out tracts in almost all patients. The excluded tracts presented with unrealistic trajectories.

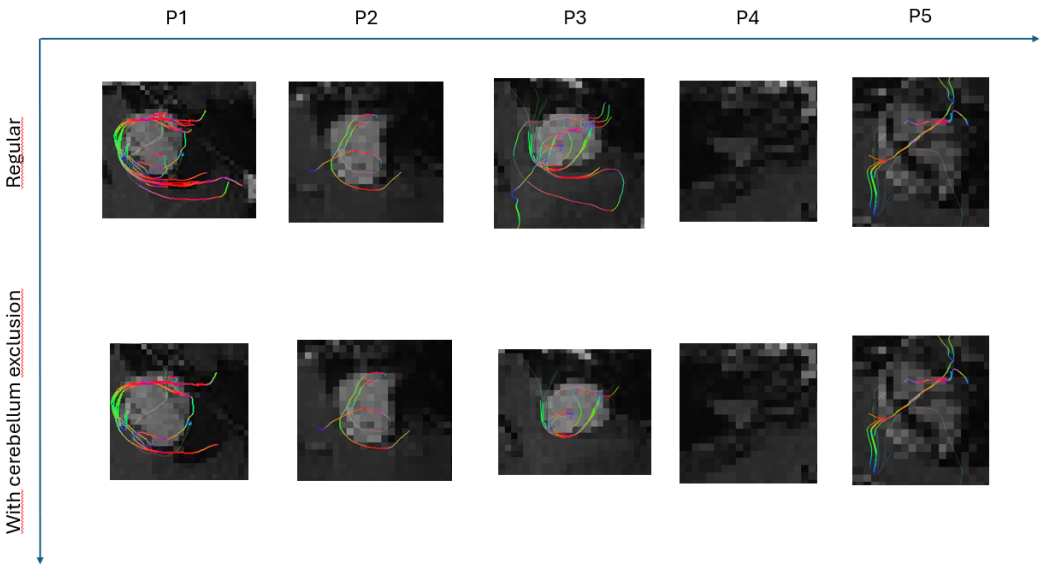

Figure 17: tractography results with and without the usage of a cerebellar exclusion ROI.

Discussion

We were able to reconstruct tracts using the different parameter combinations in all patients except one. The parameter selection was consequently not based on the results of this patient.

We saw no results in patient 4 for any parameter combinations. This patient had a relatively small lesion, which was located intracanicular. Consequently, the tumor ROI was also located intraossal. We expect that susceptibility artefacts negatively impacted the diffusion signal and consequently hindered tract reconstruction in this patient [38]. After surgery, it was also revealed that the tumor was a meningioma. Combined with the other factors, we decided to exclude the results of this patients.

Based on the results of the four remaining patients, a combination of an FA value of 0.1 and an angle threshold of 35 degrees would be optimal. However, we expect that this might be too strict when considering new patients. Additionally, the reduction in false-positives was minimal for this parameter combination when comparing it to one step more lenient. We therefore decided to use an FA value of 0.1 and an angle threshold of 40 degrees throughout our study.

The addition of the cerebellar exclusion ROI only excluded tracts with unrealistic trajectories, making the results more specific. Consequently, we decided to use this ROI in the main part of the study.

Conclusion

Based on the tractography results in five VS patients, we conclude that a combination of an FA threshold of 0.1 and an angle threshold of 40 degrees, combined with the cerebellar ROI, is optimal for facial nerve tractography in patients with vestibular schwannomas.

3. Questionnaire tractography in the OR

Circle the number that represents to which extent you agree with the statement (1: totally disagree, 5: totally agree).

The facial nerve location in the 3D model corresponds to the intraoperative location.

1 2 3 4 5

The method changed my expectation of the facial nerve location.

1 2 3 4 5

The method is beneficial for my understanding of the expected intraoperative facial nerve location.

1 2 3 4 5

The method is beneficial for the treatment of patients.

1 2 3 4 5

The method is useful in the preoperative setting.

1 2 3 4 5

This method can make the surgery faster.

1 2 3 4 5

It was easy to translate the information from the imaging to the intraoperative setting.

1 2 3 4 5

It is necessary to register the hologram onto the patient to fully exploit the benefits of the preoperative facial nerve localization.

1 2 3 4 5

The visualisation method (2D, 3D) is important for my understanding of the data.

1 2 3 4 5

I think that further improvements are necessary before clinical implementation.

1 2 3 4 5

Explanation of answers: